

Computation of Transonic Flow Around Airfoils with Trailing Edge and Shock/Boundary Layer Interactions

M M S Khan*

Lockheed-Georgia Company Marietta, Georgia

G R Inger†

University of West Virginia Morgantown West Virginia

and

S G Lekoudis‡

Georgia Institute of Technology, Atlanta, Georgia

A viscous/inviscid interaction procedure is developed for computing steady transonic flows over single airfoils. It combines the method used in the GRUMFOIL code with a solution for transonic shock/boundary layer interactions. For airfoil shock locations around midchord it was found that marching under the shock using boundary layer theory gives results which are similar to those obtained with a detailed interaction theory except for significant changes in the prediction of displacement thickness rise and skin friction drop downstream of the shock. However, the two procedures give significantly different results when the shock position is rearward (70% chord or more). Then the shock/boundary layer interaction module alters the flow with consequent global effects on shock location and lift.

Nomenclature

C	= airfoil chord
C_E	= entrainment function = $1/\rho_e u_e (d/ds)$ ($\rho_e u_e H_1$)
C_F	= skin friction coefficient
C_p	= pressure coefficient
C_L	= lift coefficient
C_D	= drag coefficient
C_M	= moment coefficient
H_i	= "incompressible" shape factor
H_1	= $\delta - \delta^* / \theta$
M	= Mach number
Re_c	= Reynolds number based on chord
S	= surface coordinate
α	= angle of attack
δ^*	= displacement thickness
θ	= momentum thickness
ρ	= density
ν	= kinematic viscosity

Subscripts

A B C D O	= related to streamwise locations around the shock
e	= boundary layer edge conditions
∞	= freestream conditions

Introduction

THE transonic flow around airfoils can be influenced to a large degree by viscous effects.¹ Thus, detailed design of such airfoils requires the capability of accurately predicting the viscous effects. There are two ways of obtaining this capability, both being pursued vigorously. The first is to solve

the two dimensional Navier Stokes equations for the whole flowfield. Although this is the most complete model, it needs significant computer resources because of the stringent requirements of adequate resolution of different parts of the flowfield. The second way of obtaining the predictive capability is through a composite approach involving viscous/inviscid interactions. This way, solutions of different parts of the flowfield are combined in an iterative scheme. The scheme updates these solutions until convergence criteria are satisfied. Thus, the simplifying approximations appropriate to the different parts of the flowfield can be used to compute solutions efficiently. Reference 1 contains a number of different approaches and areas of application of viscous/inviscid interactions. In paper 15 of Ref. 1, a simplified procedure due to Murman is used to account for shock/boundary layer interactions.

In general, the segmentation of the different areas of the flowfield is done according to the importance of viscosity. A classical segmentation is between inviscid parts of the flowfield, usually treated with a potential, and areas where the thin shear layer equations apply, the boundary layer and the wake. However, segmentation does not account for regions of the flowfield where both the streamwise pressure gradients and the role of viscosity are important simultaneously. For the transonic flow around airfoils, such regions can be the shock/boundary layer interaction (SBLI) region and the trailing edge region. These regions are usually called the strong interaction regions.

The importance of these two regions has been examined before, but for each region individually. Reference 2 describes a code named GRUMFOIL that computes the steady transonic flow around airfoils using a lag entrainment solution for the turbulent boundary layer. It also uses a special solution for the turbulent flow around the trailing edge that accounts for the strong interactions that occur in that region. Boundary layer theory is used to march under the shock. The code has been validated at Lockheed Georgia.³ It was found that the code produces satisfactory agreement with the experiments for subcritical cases. It was also found that sometimes, excessive Mach number corrections were needed to move the shock forward so that satisfactory agreement could be produced for supercritical cases. The effects of the tunnel walls in transonic flow does cloud the issue when

Presented as Paper 82-0989 at the AIAA/ASME 3rd Joint Thermophysics, Fluids, Plasma and Heat Transfer Conference, St. Louis, Mo., June 7-11, 1982; submitted July 2, 1982; revision received Dec 12, 1983. Copyright © American Institute of Aeronautics and Astronautics, Inc., 1982. All rights reserved.

Associate Scientist, Department 72/74, Member AIAA.

†Professor, Department of Mechanical and Aerospace Engineering, Associate Fellow AIAA.

‡Associate Professor, School of Aerospace Engineering, Member AIAA.

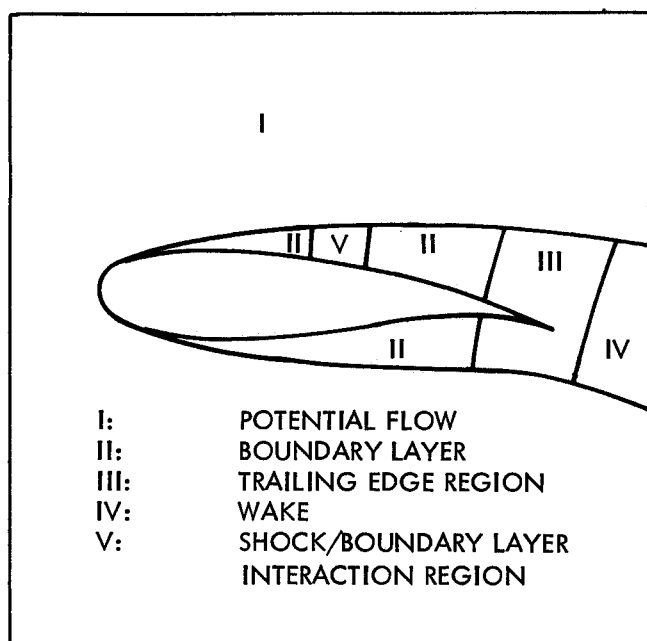


Fig 1 Schematic of the segmentation of the flowfield around a single airfoil

comparison with experiments is attempted. Because of this problem, no comparison with the experiments will be attempted in this paper.

The question that this work addresses is the following: what is the combined influence of the strong interactions which occur at the trailing edge and the shock/boundary layer interaction region in the prediction of the unseparated viscous transonic flow around isolated airfoils? The tools used in answering this question are: the GRUMFOIL code and the shock/boundary layer interaction theory of Inger.^{4,5} The procedure used maintains the attractive features of viscous/inviscid coupling: good numerical resolution of the separately computed regions of the flow and fast execution on the computer. Briefly, the procedure works as follows. The GRUMFOIL code was modified so that the turbulent boundary layer calculations are discontinued in the shock region. The interaction theory of Inger is used to generate the boundary layer quantities after the shock region where the boundary layer calculations are reinitiated. It is also used in the shock region to generate the entrainment velocities required for the viscous/inviscid coupling. Details of the procedure are given next.

The Viscous/Inviscid Interaction Procedure

The viscous/inviscid interaction procedure described in this paper is based on incorporating a shock/boundary layer interaction module in the GRUMFOIL code. A schematic of the segmentation of the flowfield is given in Fig 1.

The inviscid part of the flow is computed using a conservative form of the full potential equation.² Thus, isentropic flow was assumed across the shock. This is inappropriate for strong shocks, and for the airfoils examined an error estimate is provided in GRUMFOIL. Consider the last supersonic point and downstream of it, the first subsonic point in the shock region of the potential flow grid. The pressure coefficient produced by the isentropic assumption at the subsonic point differs by less than 10% from the pressure coefficient generated using the Rankine-Hugoniot relationships. This happened at the airfoil surface. (The quotation marks indicate that the actual solution includes the displacement effects of viscosity.) The total change in the pressure coefficient across the shock is greater than the difference between the pressure coefficients at the two mesh

points mentioned, sometimes more than twice as large. Thus, although the preshock Mach number in the cases examined was never higher than 1.3, the possible error introduced by the isentropic approximation could be comparable to the changes stemming from different treatment of the flow at the root of the shock. This error warrants further study using the Euler equations. No smoothing of the pressure distribution has been used in any of the calculations reported in this paper. Both first and second order differencing was tried for the supersonic regions. Practically no differences were found in the answers.

A form of the kinetic energy equation for thin shear layers is used to generate an ordinary differential equation for the entrainment function C_E in GRUMFOIL.⁶ Neither the boundary layer theory nor the approximations used in the kinetic energy equation are capable of handling very large adverse streamwise pressure gradients or non-negligible pressure gradients normal to the airfoil surface. The reason for this study is not only the incorrect flowfield that might be computed by the boundary layer equations at the root of the shock, but the influence of the shock on the subsequent development of the boundary layer.

The method used to compute the shock/boundary layer interaction region for weak shocks was developed by Inger⁴ using a nonasymptotic solution of the linearized Navier-Stokes equations. The solution has been expressed in a parametric form,⁵ the required input to the theory being the incoming boundary layer displacement thickness, Reynolds number, the incompressible shape factor, and the preshock Mach number. The theory then gives the pressure and skin friction distributions across the interaction zone, along with estimates of the extent of the interaction zone.

In GRUMFOIL, the coupling between the inviscid part of the flow and the viscous parts is done by using the transpiration velocity. This velocity is computed from flow variables generated by the lag entrainment method. Thus, in order to insert a local solution for the shock/boundary layer interaction region, the solution must be used to compute the transpiration velocity in the interaction region. This was done in the present study. However, before the insertion is accomplished, the location and the extent of the interaction region has to be determined.

Computing the Region of the Shock/Boundary Layer Interaction

Because the boundary layer theory is not used under the shock, the ends of the interaction region have to be determined. The potential flow calculation and the viscous/inviscid coupling produce a smeared shock. Thus, the ends of the interaction region can be defined in a nonunique manner. There are two guides for their definition. The first is that the boundary layer calculations should not be subjected to the pressure rise at the shock. The second is the extent of the interaction region given from the interaction theory for the particular combination of the incoming boundary layer properties and the preshock Mach number. It turns out that unless the Reynolds number based on the airfoil chord and the freestream velocity is below a million, the computed interaction length is shorter than the smeared shock width at the airfoil surface. Thus, the requirement that the boundary layer not be subjected to the pressure rise at the shock is used to determine the ends of the interaction zone.

A schematic of the distribution of the pressure coefficient in the shock region is shown in Fig 2. The mesh points A and B satisfy the above discussed requirements about the ends of the interaction zone. Considerable experimentation was done to determine a reliable way of finding the points A and B. These points vary in location during the iterative viscous/inviscid coupling. The point O is named the root of the shock in the potential flow grid. It was found that the results are not very sensitive to the location of O as long as O is between A and B. Thus, the following procedure was used to locate the interaction region.

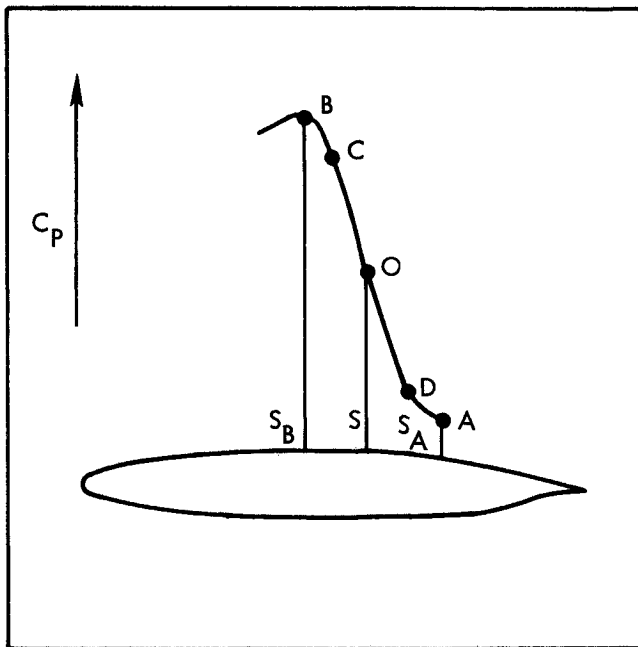


Fig 2 Schematic of location of the shock/boundary layer interaction region

The point O was defined as the last supersonic point in the potential flow calculation. The points A and B next to the neighboring points C and D, downstream and upstream of the point O, respectively, were taken as the ends of the interaction region. However, if the ratio

$$\frac{(C_p)_A - (C_p)_D}{(C_p)_D - (C_p)_O} \quad (1)$$

and/or the ratio

$$\frac{(C_p)_A - (C_p)_C}{(C_p)_C - (C_p)_O} \quad (2)$$

was less than a prescribed quantity, the point D and/or the point C marked the ends of the interaction region. Numerical experiments showed that 0.1 was a good value for the prescribed ratio and reliably produced the interaction region. Thus, the interaction region ranged from three to five points in the potential flow grid.

The interaction theory gives a continuous variation of the boundary layer parameters in the interaction region. The interaction theory provides this variation in a parameterized form of smooth exponential relations using the upstream boundary layer parameters and the characteristic upstream and downstream lengths of the SBLI region. A schematic of this variation is shown in Fig 3. The calculation of the potential flow requires boundary layer quantities only at the discrete points. At these points the boundary layer parameters are computed using the continuous parameterized form of the interaction solution. There were two other alternatives for treating the intermediate points C and D of Fig 2. The first is to keep the boundary layer quantities "frozen" and equal to the end values. The second alternative is to use interpolated values between the values at the root of the shock (point O) and the values at the ends of the interaction region (points A and B). Both options were used. It was found that the results were practically insensitive to the choice.

A test was performed to study the sensitivity of the results to the form of the interpolation. Both linear and exponential variation were assumed for the boundary layer properties in the interaction region; the latter because, according to the

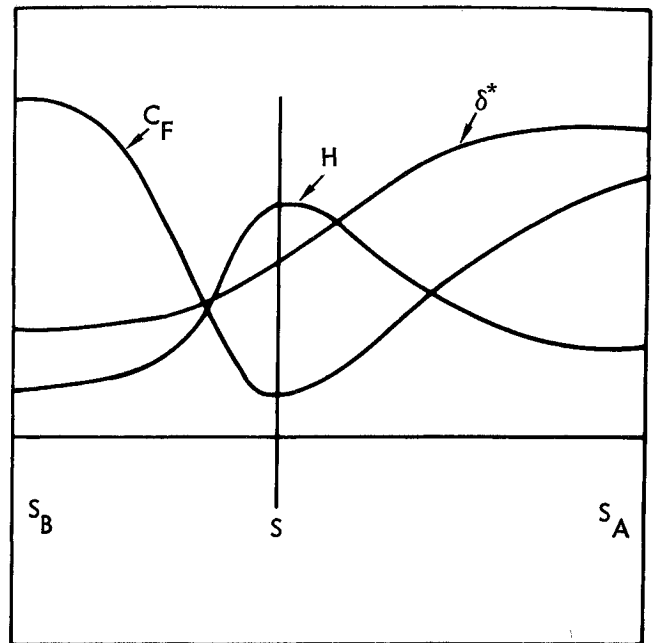


Fig 3 Schematic variation of quantities in the shock/boundary layer interaction region

interaction theory (Fig 3) the streamwise variation of the properties is negligible at the ends of the interaction region. The change in integral parameters like C_L , C_D , C_M and the shock location was affected by about 1% from the change in the type of the interpolation.

Another test was performed in order to study the sensitivity of the results to the extent of the interaction region. The boundary layer properties were kept "frozen" and equal to the values at point A at the next location downstream of point A. It was found again that the resulting integral parameters like C_L , C_D , C_M and the shock location were practically insensitive to that change. Furthermore, all the values of the boundary layer properties at C and D were found using the parameterized form of the interaction solution.

The Viscous/Inviscid Coupling

A grid sequencing is used in the potential flow calculation in GRUMFOIL. The number of points used in the "wraparound" direction is 40, 80, and 160 as the grid becomes denser. In order to save time, the shock/boundary layer interaction is computed only in the dense grid. In the two coarse grids, boundary layer theory is used to march under the shock. There was no increase in the number of relaxation cycles necessary to converge, nor was there a need to change the relaxation parameters. As a result, there is practically no change in the run time of GRUMFOIL.

A parameter that affects the solution significantly in the shock region is the entrainment function C_E . Relationships based on its definition are given in the Appendix. In the lag entrainment system, C_E is a dependent variable related empirically with the kinetic energy of turbulence. The distinction between "equilibrium" and "nonequilibrium" values of C_E is used in formulating the lag entrainment system. An effective inviscid injection velocity v_i (a relationship expressing its definition is given in the Appendix) is computed in GRUMFOIL using the entrainment function and the external streamwise velocity distribution at the boundary layer edge. Since the interactive pressure gradients play an important role in determining these parameters, both C_E and v_i are explicitly computed from the boundary layer parameters given by the interaction theory. Because only the basic definition of C_E is used (see Appendix), there is no need to distinguish between its equilibrium and nonequilibrium

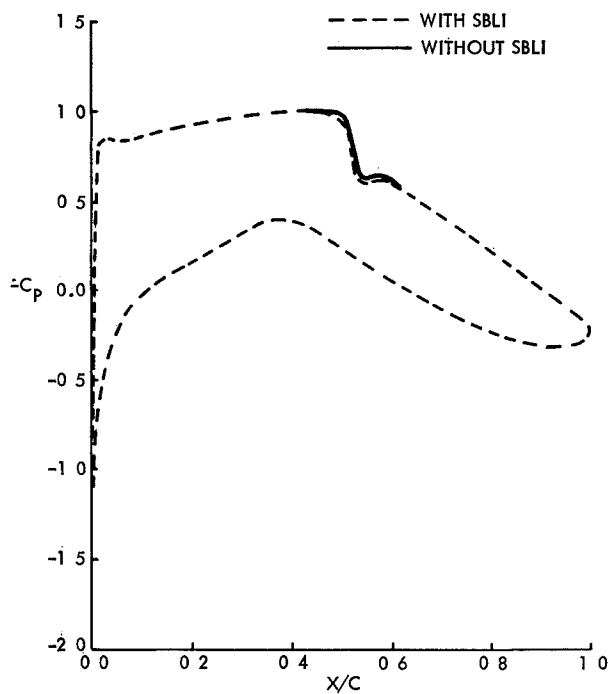


Fig 4a Predicted pressure distribution for the RAE 2822 airfoil $M_\infty = 0.730$ $\alpha = 1.704^\circ$ $Re = 6.5 \times 10^6$

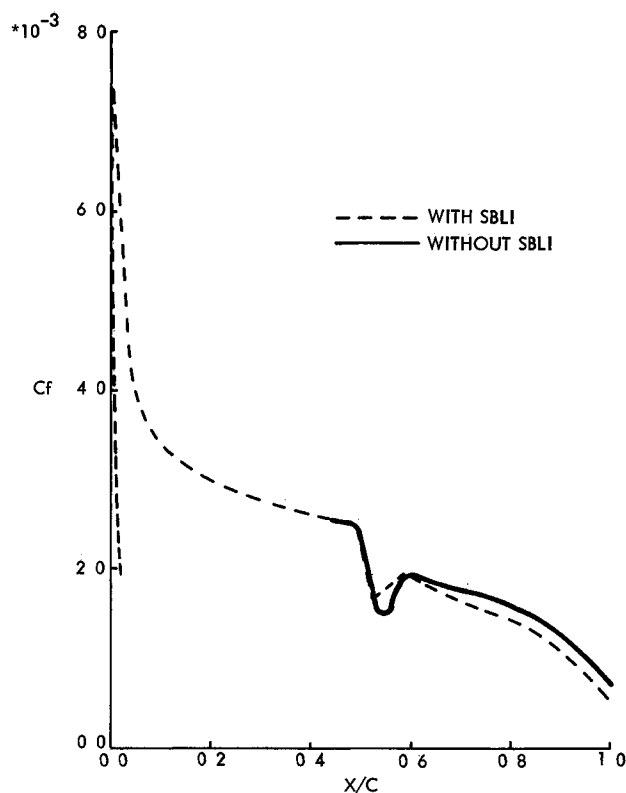


Fig 4c Predicted skin friction distribution for the upper surface of the RAE 2822 airfoil $M_\infty = 0.730$ $\alpha = 1.704^\circ$ $Re = 6.5 \times 10^6$

values. Generally it was found that the interaction theory gives lower values for C_E in the region after the shock than for the lag entrainment method.

Results

This extended composite flowfield analysis method has been applied to the study of numerous supercritical airfoils. Several selections from these results, which illustrate the salient SBLI effects of interest, will now be presented and discussed.

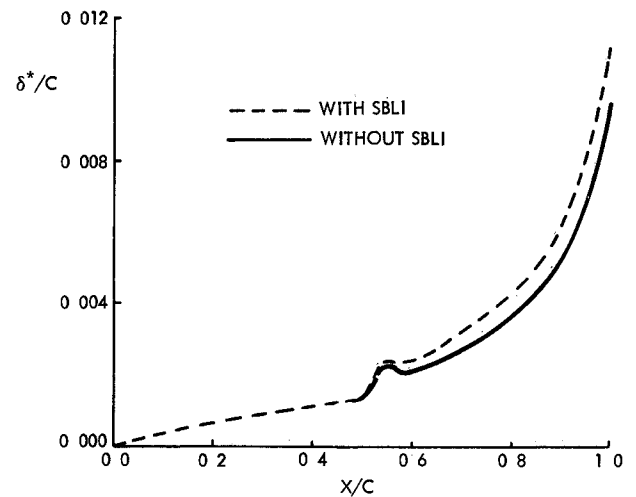


Fig 4b Predicted displacement thickness distribution for the upper surface of the RAE 2822 airfoil $M_\infty = 0.730$ $\alpha = 1.704^\circ$ $Re = 6.5 \times 10^6$

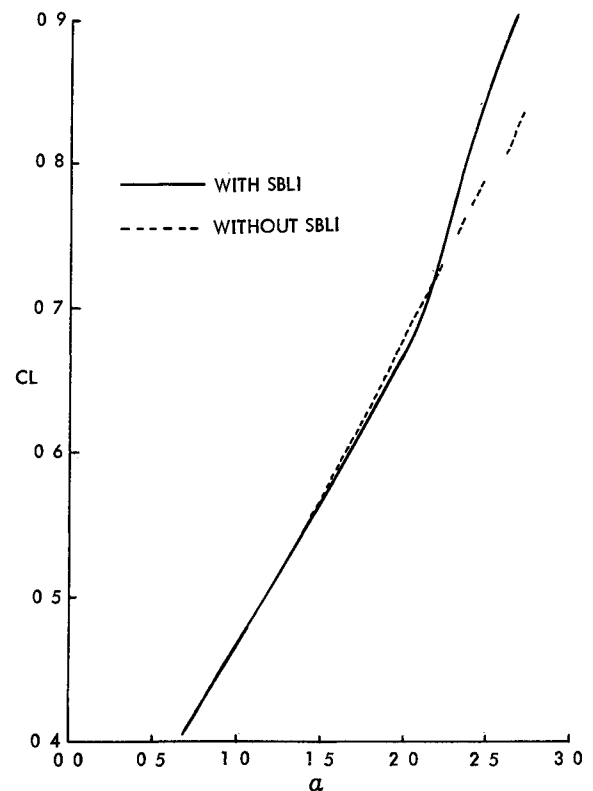


Fig 5 Predicted C_l α curve for the RAE 2822 airfoil $M_\infty = 0.730$ $Re = 6.5 \times 10^6$

RAE 2822

We consider first the experimentally documented RAE 2822 airfoil, which is a widely cited check case. The predicted pressure, displacement thickness and skin friction distributions for a typical cruise flight condition are illustrated in Figs 4a-c. As expected for this moderately aft loaded condition with a relatively forward shock position around midchord ($0.50 < x_{SH}/c < 0.60$), the two ways of computing the SBLI effect yield almost identical results for the pressure distribution and shock location. However, the detailed interaction effects on δ^* and C_F are more important; improper treatment of the interaction zone can underpredict the subsequent δ^* increase and C_F drop. The effect of SBLI becomes more pronounced at higher angles of attack.

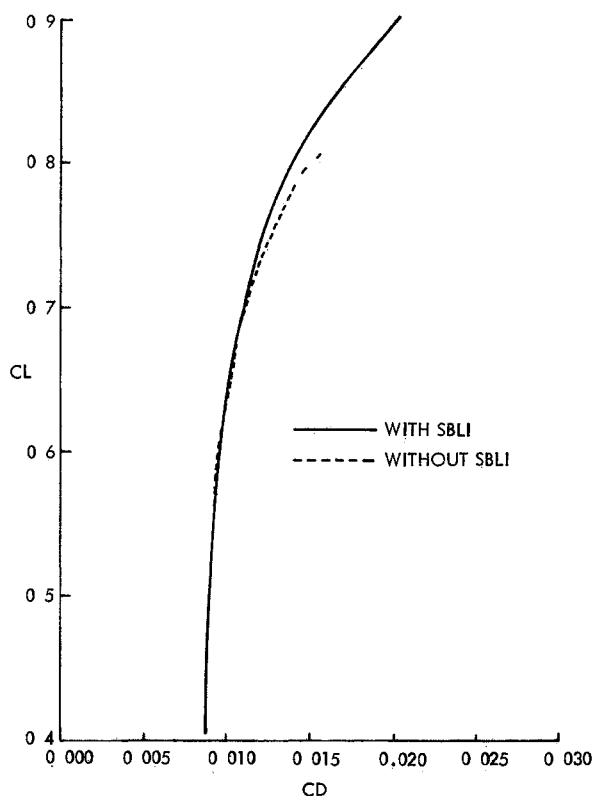


Fig 6 Predicted drag polar for the RAE 2822 airfoil $M_\infty = 0.730$ $Re = 6.5 \times 10^6$

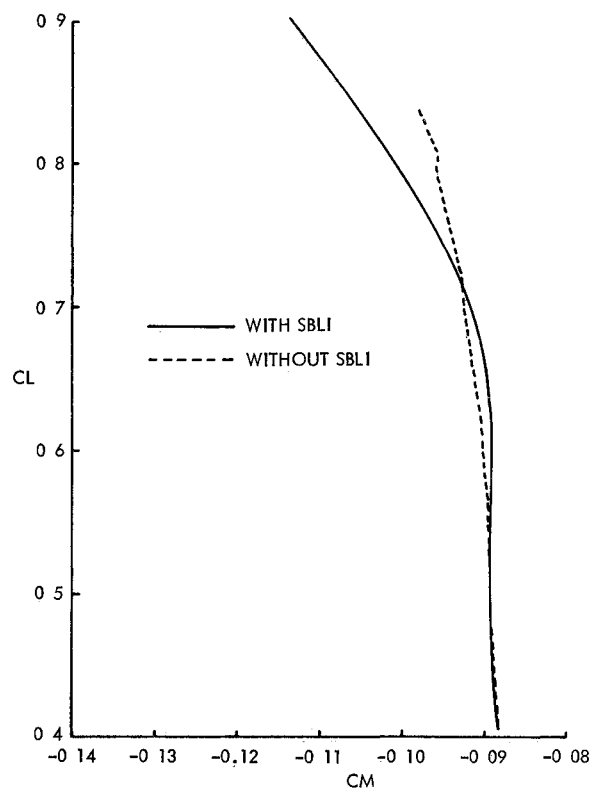


Fig 7 Predicted C_L C_M curve for the RAE 2822 airfoil $M_\infty = 0.730$, $Re = 6.5 \times 10^6$

An extensive parametric study of a wide range of operating conditions was done to evaluate the relative SBLI modeling effect on the global aerodynamics of this typical airfoil. The results for typical full scale Reynolds number and flight Mach number, deemed a significant aspect of the present investigation, are presented in the form of the predicted lift curves C_L vs α (Fig 5), drag polars C_D vs C_L (Fig 6), and the associated pitching moment characteristics C_M vs C_L (Fig 7). It is clearly seen from Fig 5 that the global influence of the SBLI zone detail on lift, while negligible at lower α , has an appreciable effect at higher angles of attack approaching the stall. At these higher α 's neglect of the proper SBLI modeling results in 10-15% underestimate of the lift, which is a big effect. The reason may be ascribed to the rearward movement and strengthening of the shock with increasing α , which consequently increases the global influence of the SBLI model on this very shock position and strength.

There is also an accompanying slight reduction in the predicted drag coefficient of 10 to 20 counts (Fig 6) with an attendant significant increase in the nose down pitching moment (Fig 7). It is reemphasized here that the correct trailing edge interaction is included in all these results.

The predicted effects of Reynolds number ("scale effect") on these results, which is of great practical interest to both R&D and design engineers, were also obtained in our study. These effects are weak over the examined range $6 < Re_c \times 10^6 < 30$. In all cases we see once again that the SBLI details can significantly alter the displacement thickness and skin friction well downstream of the interaction zone. This is in agreement with the earlier inferences of Inger⁷ and the recent results of Nandan et al.⁸ The evolution of the pressure distribution with the angle of attack is shown in Fig 8.

Lockheed LG4 612

As a second case study example, a 12% thick supercritical airfoil design⁹ was chosen because there is a Lockheed

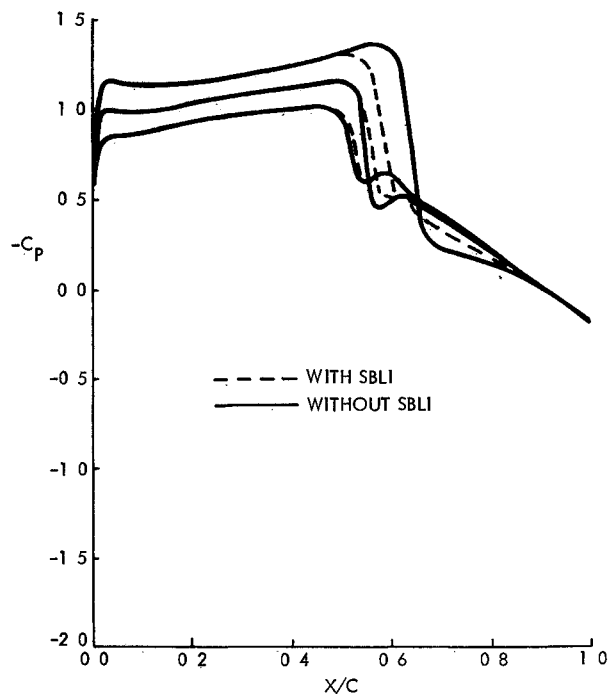


Fig 8 Predicted evolution of the pressure distribution on the RAE 2822 airfoil $M_\infty = 0.730$ $\alpha = 1.704, 2.2$ and 2.6 deg $Re = 11 \times 10^6$

Georgia experimental program aimed at measuring the flow properties in its SBLI region.¹¹ The operating cruise conditions intended for this design involve nonseparating flow at somewhat higher flight Mach numbers than the RAE 2822 and hence much more rearward shock locations ($0.60 < x_{SH}/c < 0.80$). Accordingly, one would expect significant global as well as local SBLI effects to occur at much lower angles of attack.

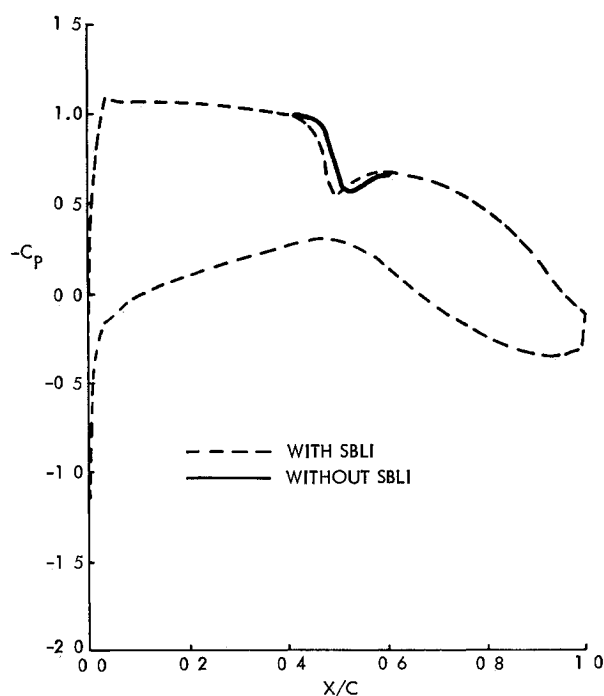


Fig 9a Predicted pressure distribution on the LG 4 612 airfoil $M_\infty = 0.735$ $\alpha = 1.462$ deg $Re = 11 \times 10^6$

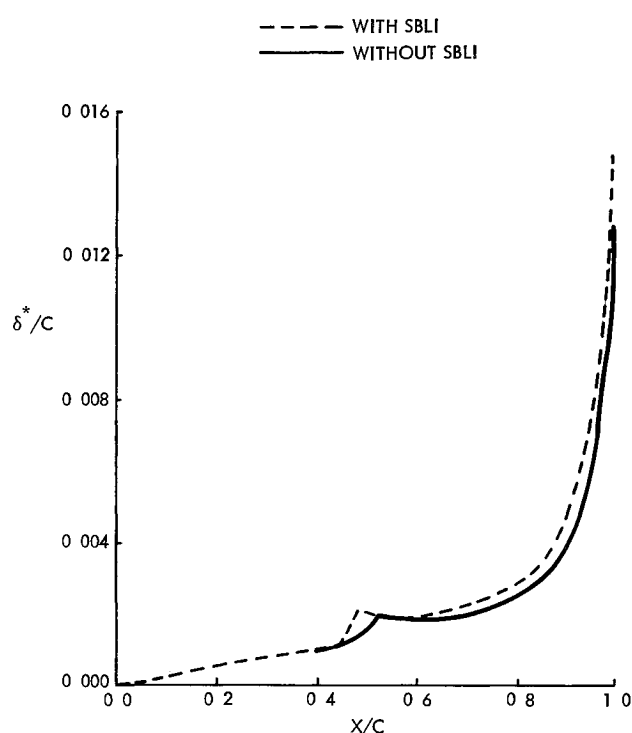


Fig 9b Predicted displacement thickness distribution for the upper surface of the LG4 612 airfoil $M_\infty = 0.735$ $\alpha = 1.462$ deg $Re = 11 \times 10^6$

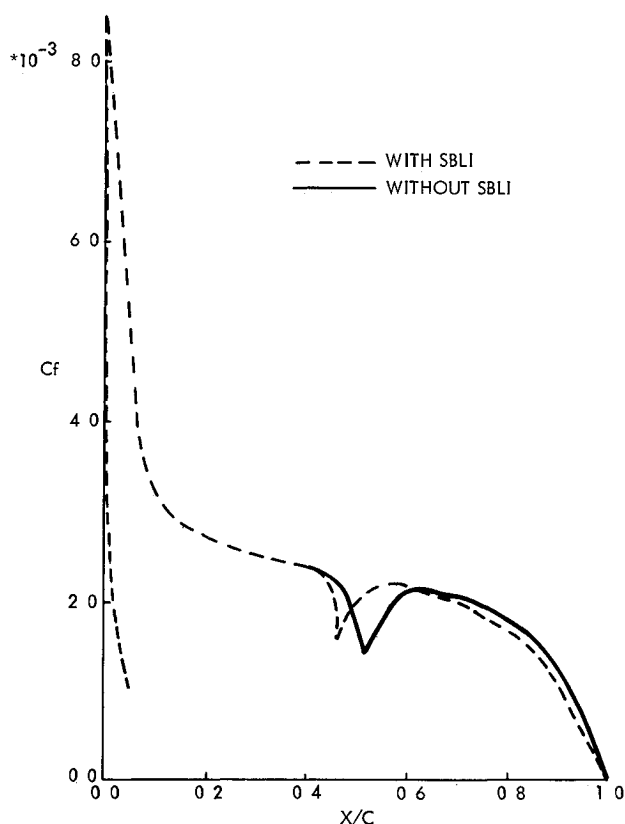


Fig 9c Predicted skin friction distribution for the upper surface of the LG4 612 airfoil $M_\infty = 0.735$ $\alpha = 1.462$ deg $Re = 11 \times 10^6$

Typical pressure displacement thickness and skin friction distribution predictions for this airfoil at an $M_\infty = 0.735$ $Re_c = 11 \times 10^6$ flight condition are presented here for two angles of attack a moderate cruise angle $\alpha = 1.46$ well below stall onset (Figs 9a c) and a higher $\alpha = 2.0$ deg in the stall onset (Figs 10a c). As expected the global influence of the SBLI module is significant in altering the shock location and strength even at the lower α condition and is quite

pronounced indeed at $\alpha = 2.00$ deg. This is further borne out by parametric study results over a range of α for the global aerodynamic coefficients presented in Figs 11 13. There is a 10 15% relative lift and negative pitching moment enhancement with increasing angle of attack predicted by the inclusion of the proper SBLI zone modeling.

Concluding Remarks

A fundamentally based shock/boundary layer interaction module has been incorporated into the state of the art viscous/inviscid coupling procedure GRUMFOIL, which computes the steady unseparated transonic flow around single airfoils including the trailing edge interaction region.

For nonseparating airfoil operating conditions involving shock locations around midchord (such as a low angle of attack and moderate Mach number cruise flight condition) it was found that inclusion of proper modeling of the shock/boundary layer interaction has little influence on the global aerodynamic properties although it does result in noticeable errors in the predicted displacement thickness and skin friction distributions for distances downstream of the shock. However for airfoils that operate at higher angles of attack and/or Mach number (such as approaching incipient stall) where a more rearward (70% chord or more) shock locations occur the details of the SBLI zone exert significant global effects on lift (10 15%) drag and pitching moment as well as very noticeable local flowfield effects. These results are in agreement with the qualitative implications of several earlier studies. More results from the code developed in this work are found in Ref 10.

As a broad rule of thumb it is the conclusion of this study that when the shock is more than about 60% chord aft the proper details of the shock/boundary layer interaction zone should be included for accurate aerodynamic predictions as well as local boundary layer flow results downstream. When this is done the resulting modified GRUMFOIL composite code should yield good results (including the incipient stall regime) up to the point of boundary layer separation in the trailing edge region.

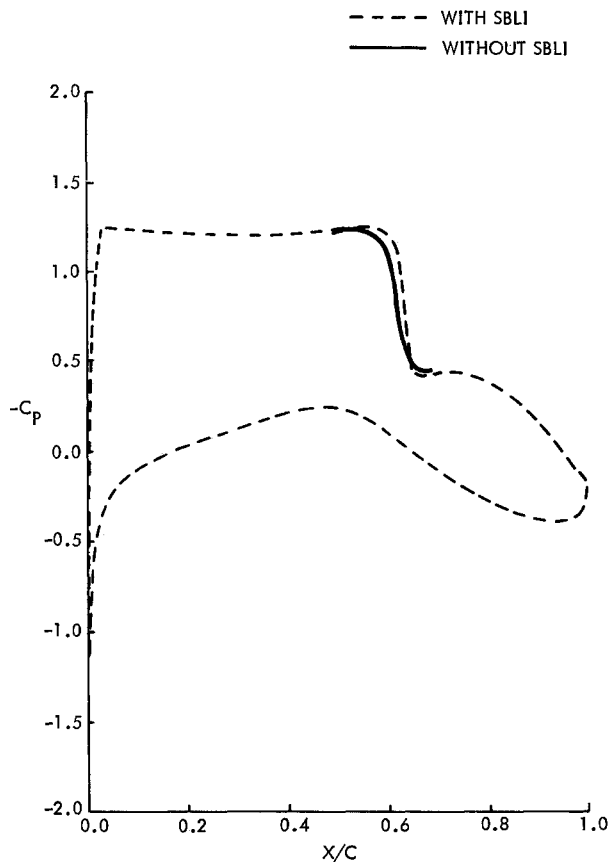


Fig. 10a Predicted pressure distribution on the LG4-612 airfoil. $M_\infty = 0.735$, $\alpha = 2.00$ deg, $Re = 11 \times 10^6$

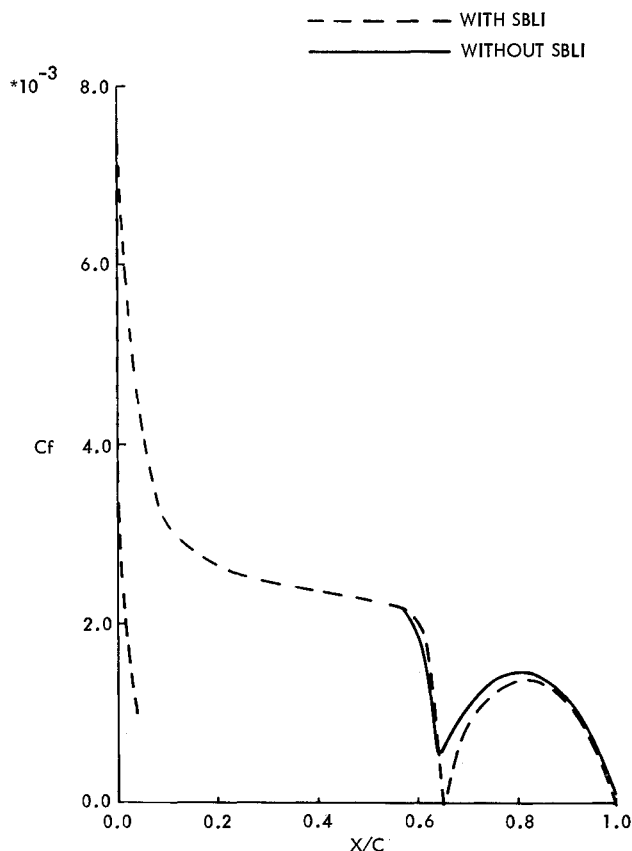


Fig. 10c Predicted skin friction distribution for the upper surface of the LG4-612 airfoil. $M_\infty = 0.735$, $\alpha = 2.00$ deg, $Re = 11 \times 10^6$

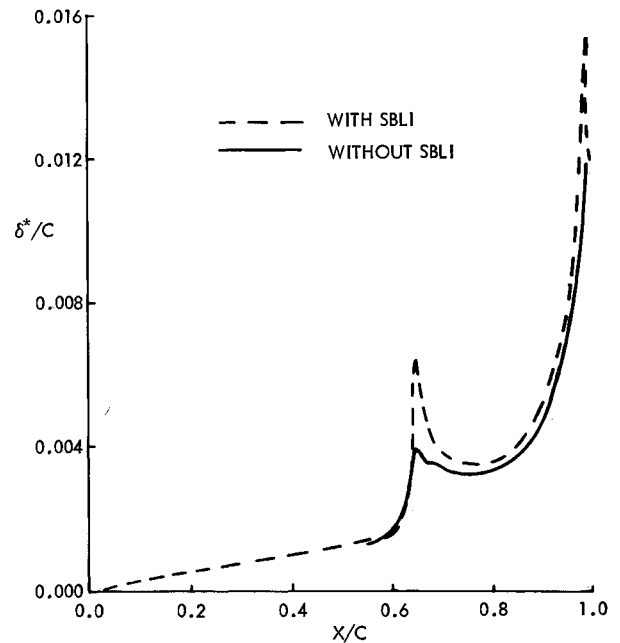


Fig. 10b Predicted displacement thickness distribution for the upper surface of the LG4-612 airfoil. $M_\infty = 0.735$, $\alpha = 2.00$ deg, $Re = 11 \times 10^6$

Appendix

The entrainment function C_E is defined as

$$C_E = \frac{l}{\rho_e u_e} \frac{d}{dx} \int_0^\delta \rho u dy \quad (A1)$$

From the integrated continuity equation across the boundary layer, the streamline slope at the boundary-layer edge is formally linked to this function by the general relationship

$$\frac{V_e}{U_e} = -C_E + \frac{d\delta}{dx} \quad (A2)$$

The strong influence of C_E on the inviscid transpiration velocity of the GRUMFOIL code is evident in Eq. (A2).

Instead of supplying an empirical formula for C_E , we may instead develop a basic relationship that links it directly to the local interaction properties, working directly from the right hand side of Eq. (A1). Thus, upon introducing the definition of displacement thickness δ^* we have

$$C_E = \frac{d(\delta - \delta^*)}{dx} + (\delta - \delta^*) \frac{d\ln}{dx} (\rho_e U_e) \quad (A3)$$

Then subtracting out the local C_E pertaining to the undisturbed boundary layer (denoted by subscript 0), the interactive perturbation (indicated by a prime) is given in the leading approximation for a small disturbance isentropic inviscid flow by the expression

$$C'_E \equiv \frac{d(\delta - \delta^*)}{dx} + (\delta_0 - \delta_0^*) \left(\frac{Me_0^2 - 1}{\gamma \rho_0 Me_0^2} \right) \frac{dpe'}{dx} \quad (A4)$$

since δ_0 changes negligibly along the short interaction zone. Now it can be further shown that $\delta / \delta^* \approx \delta_0 / \delta_0^*$ to the same order of approximation and Eq. (A4) yields the useful result

$$C'_E \equiv \left(\frac{\delta_0}{\delta_0^*} - 1 \right) \left[\frac{d\delta^*}{dx} + \frac{\delta_0^* (Me_0^2 - 1)}{\gamma \rho_0 Me_0^2} \right] \left(\frac{dpe'}{dx} \right) \quad (A5)$$

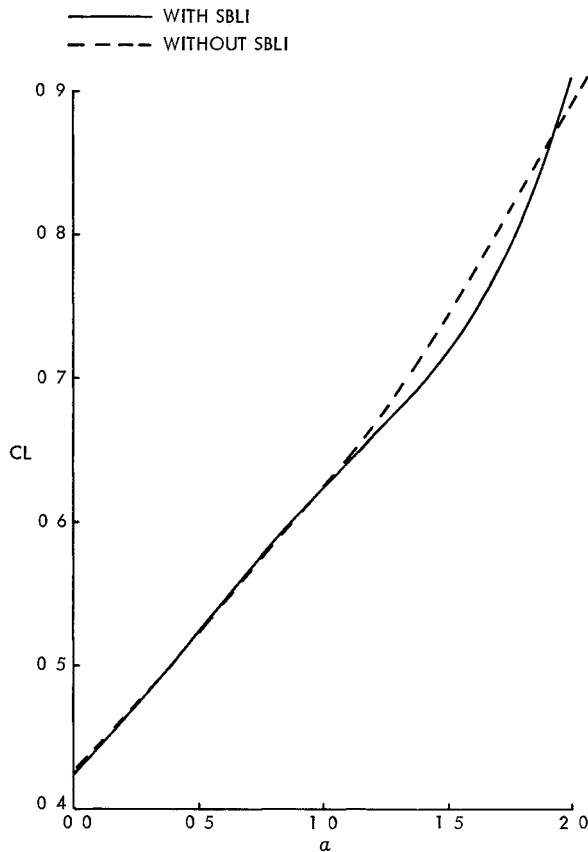


Fig 11 Predicted C_L α curve for the LG4 612 airfoil $M_\infty = 0.735$ $Re = 11 \times 10^6$

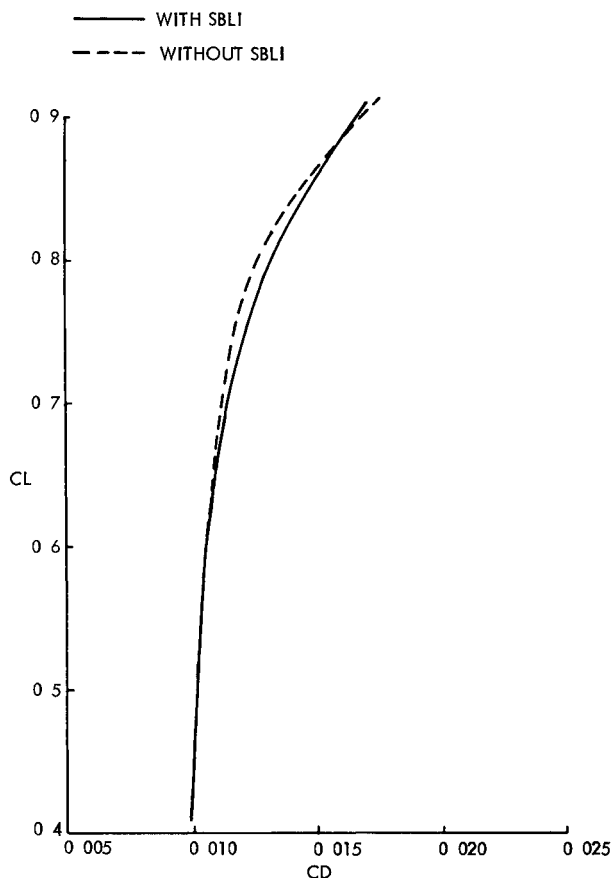


Fig 12 Predicted drag polar for the LG4 612 airfoil. $M_\infty = 0.735$ $Re = 11 \times 10^6$

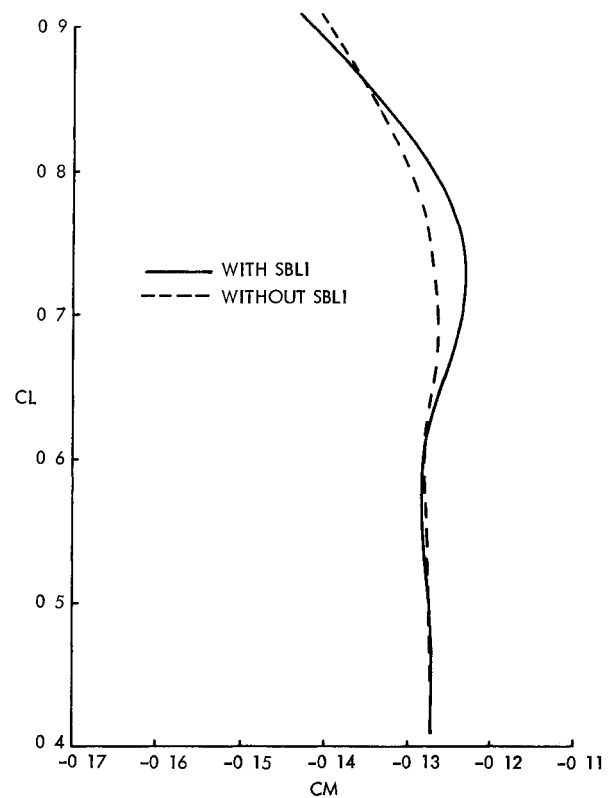


Fig 13 Predicted C_L C_M curve for the LG4 612 airfoil $M_\infty = 0.735$ $Re = 11 \times 10^6$

This relationship provides the correct local interactive change of C_E without any empiricism relating it directly to the correct interactive solutions for $\delta^*(x)$ and $pe(x)$ along with the proper incoming local undisturbed boundary layer properties. Similarly the effective inviscid injection velocity can be related directly to the correct interactive solutions for the displacement thickness and the pressure distribution as follows:

$$\frac{v_i}{U_e} \equiv \frac{I}{\rho_e U_e} \frac{d}{dx} (\rho_e U_e \delta^*) \quad (A6)$$

$$\frac{v_i}{U_{e0}} \equiv \delta_0^* \left[\frac{d}{dx} \left(\frac{\delta^*}{\delta_0^*} \right) + \frac{(Me_0^2 - 1)}{\gamma \rho_{e0} Me_0^2} \left(\frac{dpe}{dx} \right) \right] \quad (A7)$$

Equation (A5) typically predicts a maximum $C'_E > 0$ around the shock foot station of the interaction zone

Acknowledgments

This work was supported by Lockheed Georgia's IR&D program. The third author was supported by a grant from the Advanced Research Organization of the Lockheed Georgia Company. The help of Harry Mead of Grumman in understanding some of the internal structure of GRUMFOIL is appreciated.

References

- ¹ Computation of Viscous/Inviscid Interactions AGARD Conference Proceedings No 291 1981
- ² Melnik R E Turbulent Interaction of Airfoils at Transonic Speeds—Recent Developments, AGARD CP 291 1981 Paper 10
- ³ Ragab S and Lekoudis S G, Validation of the GRUMFOIL Computer Code Lockheed Georgia Co Marietta Ga Engineering Report ER0093 1981

⁴Inger G R Transonic Shock Turbulent Boundary Layer Interaction and Incipient Separation on Curved Surfaces ' *Journal of Aircraft* Vol 20 June 1983 pp 571 574

⁵Inger G R Some Features of a Shock Turbulent Boundary Layer Interaction Theory in Transonic Flowfields AGARD CP 291 1981, Paper 18

⁶Green J E Weeks D J and Brooman J W F Prediction of Turbulent Boundary Layers and Wakes in Compressible Flow by a Lag Entrainment Method RAE Technical Report 72231 Dec 1973

⁷Inger G R Application of a Shock Turbulent Boundary Layer Interaction Theory in Transonic Flowfield Analysis *Transonic*

Aerodynamics Vol 81 of *Progress in Astronautics and Aeronautics* AIAA New York 1982 pp 621 636

⁸Nandan M, Stanewsky E and Inger G R Airfoil Flow Analysis with a Special Solution for Shock/Boundary Layer Interaction, *AIAA Journal* Vol 19 Dec 1981 pp 1540 1546

⁹Keable F and Smith P R High Reynolds Number Test of a 12 Percent Thick Supercritical Airfoil Lockheed Georgia Co Marietta Ga Rept LG5ER0147, 1975

¹⁰Khan M M S and Dean P D The Aerodynamic Effects of SBLI on Selected Supercritical Airfoils Lockheed Georgia Co Marietta Ga Engineering Rept ER0173 1982

From the AIAA Progress in Astronautics and Aeronautics Series

AEROACOUSTICS:

JET NOISE, COMBUSTION AND CORE ENGINE NOISE—v 43

FAN NOISE AND CONTROL, DUCT ACOUSTICS, ROTOR NOISE—v 44

STOL NOISE, AIRFRAME AND AIRFOIL NOISE—v 45

ACOUSTIC WAVE PROPAGATION,

AIRCRAFT NOISE PREDICTION,

AEROACOUSTIC INSTRUMENTATION—v 46

Edited by Ira R. Schwartz, NASA Ames Research Center; Henry T. Nagamatsu, General Electric Research and Development Center; and Warren C. Strahl, Georgia Institute of Technology

The demands placed upon today's air transportation systems in the United States and around the world have dictated the construction and use of larger and faster aircraft. At the same time, the population density around airports has been steadily increasing, causing a rising protest against the noise levels generated by the high frequency traffic at the major centers. The modern field of aeroacoustics research is the direct result of public concern about airport noise.

Today there is need for organized information at the research and development level to make it possible for today's scientists and engineers to cope with today's environmental demands. It is to fulfill both these functions that the present set of books on aeroacoustics has been published.

The technical papers in this four book set are an outgrowth of the Second International Symposium on Aeroacoustics held in 1975 and later updated and revised and organized into the four volumes listed above. Each volume was planned as a unit so that potential users would be able to find within a single volume the papers pertaining to their special interest.

v 43—648 pp	6 x 9 illus	\$19 00 Mem	\$40 00 List
v 44—670 pp	6 x 9 illus	\$19 00 Mem	\$40 00 List
v 45—480 pp	6 x 9 illus	\$18 00 Mem	\$33 00 List
v 46—342 pp	6 x 9 illus	\$16 00 Mem	\$28 00 List

For Aeroacoustics volumes purchased as a four volume set \$65 00 Mem \$125 00 List

TO ORDER WRITE: Publications Dept AIAA 1290 Avenue of the Americas New York N Y 10019